PROPCAV'95

An International Conference
on Propeller Cavitation
to celebrate 100 years of
Propeller Cavitation Research
16th -18th May 1995
Newcastle upon Tyne
United Kingdom

Edited by

E J Glover
G H G Mitchell

Department of Marine Technology
The University
Newcastle upon Tyne

Penshaw Press
1995

Development of a Skew-Blade Shape for a Ducted Controllable Pitch Propeller System

Hans-Jürgen Heinke Ship Model Basin Potsdam (SVA), Germany

Otto Philipp Techno-Trans Rostock (TTG), Germany

Abstract

With free-running propellers, increase of the skew has long been used successfully to minimize propeller-induced pressure fluctuations. With ducted controllable pitch propellers, this blade shape was not considered because of the variation of the gap during reverse conditions. A new design of the propeller blade for a trawler features a skew of 27.5°. Comparative tests on model propellers having in the duct conventional and skew blade shapes showed that the higher skew scarcely influences cavitation properties and that thrust and tangential force pulses on the propeller blade and the pressure fluctuations induced by the ducted propeller in free run and towed condition would decrease considerably.

1. Introduction

Volkswerft Stralsund started in 1985 the production of trawler type "ATLANTIK 488" of 120 m length [1]. Until 1993, 35 vessels of this type have been delivered to the respective owners. Within the scope of development of this type of vessel, work was carried out to optimize the propulsion system. Main aspects of the propeller design were in this connection a high efficiency, a favourable cavitation behaviour and minimum vibration induced by the propeller.

It was intended to build the fishing vessel "ATLANTIK 488" with a controllable pitch propeller and a duct to achieve at towing speed (V appr. 5 to 6 knots) a high tow-rope pull and to be able to guarantee at full power output of the main machine for the free-running ship speed of about 15 knots. The ducted propeller system is designed for the "full speed" condition in consideration of a high tow-rope pull and a harmless cavitation behavior in towed operation.

To improve the development of ducted propellers considering a reduction of the danger by cavitation and excitation of vibrations, the following possibilities have been investigated:

- Increase of the number of propeller blades;
- Relief of the blade tip by change of the radial load distribution;
- Use of a non-axially symmetric duct;
- Use of a blade shape with higher skew.

After analysis of the advantages and disadvantages of the diverse measures, use of a blade shape with higher skew has been adopted as suitable measure. Experience acquired with free controllable pitch propellers [2] shows that a higher skew bears favourable effect on propeller induced vibrations without impairing the propeller efficiencies. Suitable balancing of the blades at the same time permits to reduce the blade setting moments.

2. Design of a ducted propeller with high skew

Use of a ducted controllable pitch propeller as the main propulsion element of a ship hitherto is not known. The main problem is to warrant the necessary free movement between the blade tip and the inner ring of the duct when reversing from ahead to astern. The necessary gap between the blade tip and the inner duct ring to guarantee free movement during the reversing process will be larger as the skew angle, the chord length at the blade tip and the blade pitch become higher.

The free movement requires for conventional blade shapes to increase the gap that is technologically necessary to consider constructional differences but which in turn results in higher efficiency losses. Additional efficiency losses will appear due to larger blade width and thus inevitably a larger gap will be necessary to guarantee the reversing process. A paper by van Manen [3] presents the effect of the changes in efficiency.

By inclination of the generatrix of the propeller area towards the suction side of the blade and a shifting of the blade tip in to the propeller plane, the distances of the blade tip zone from the blade rotation axis and from the propeller plane fixing the blade gap will be decreased [4].

With respect to the influence of the chord length at the blade tip on the efficiency, SVA Potsdam has proved by tests on models and measurements on natural ships that the use of Kaplan propellers yields a small improvement of efficiency in comparison with conventional propellers at high thrust load coefficients only [5]. The change of efficiency of a ducted propeller system by the use of a Kaplan blade compared with a conventional propeller with rounded off blades has been investigated systematically in [6] and results are shown in Figure 1 against the thrust loading for varying pitch ratio P/D. Having defined the coefficient for thrust loading K_{dK} the use of Figure 1 permits to estimate the influence of the blade shape on the efficiency.

$$K_{dK} = \sqrt{\frac{8}{\pi C_{TH}}} \qquad \Delta\eta = \frac{\eta_K - \eta_P}{\eta_K}$$

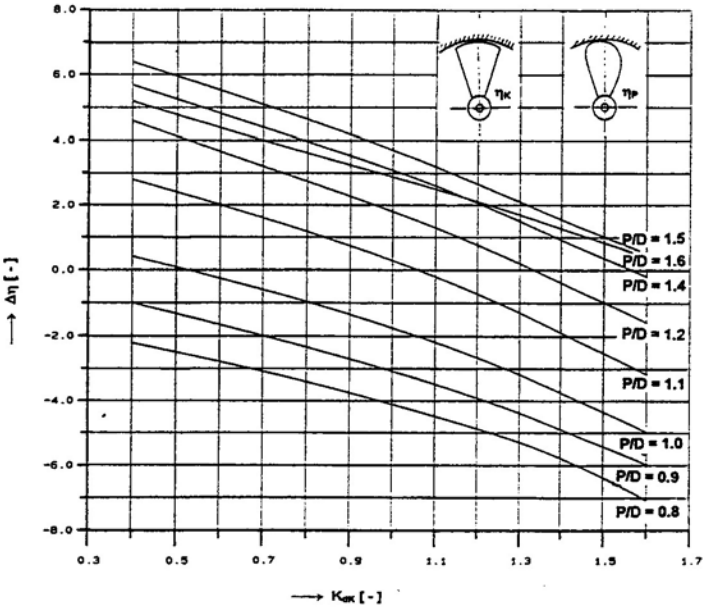

Fig. 1 Influence of the propeller blade line on the ducted propeller efficiency [6]

For the design point of the trawler a total thrust loading coefficient $C_{TH} = 2.34$ would yield a thrust loading coefficient $K_{dK} = 1.044$. As shown in Figure 1, a pitch ratio P/D = 1.10 would bear no essential influence on efficiency by the blade shape. In towed operation ($K_{dK} = 0.4$, P/D = 0.8) the influence of the blade shape is likewise small. The use of a blade shape with a disappearing chord length at the blade tip is possible.

3. Design of propeller blades

To optimise the ducted propeller a blade shape had to be designed and validated by calculation such that a suitable effective skew $\Theta_{eff} > 25°$ yields a decrease of propeller-excited pressure fluctuations and of the power and momentum fluctuations. The propeller of the Wageningen 19A duct will be designed like a free propeller subject to inflow influenced by the duct for the available power and actual speed. The hydrodynamic model is a lifting line method with corrections of the effect of the lifting surface.

Changes in the hydrodynamic method with respect to the design of a free propeller are [7]:

- Iterative fixing of the designed propeller thrust including the potential theory based calculation of the duct thrust;
- Lifting surface design calculation with induction factors for a propeller in a tube [8];
- Consideration of the duct speed induction in the propeller plane to calculate the profile inflow, cavitation numbers and variation of the wake distribution;
- Correction of the camber and of the angle of the blade profiles by the effect of the lifting surface with influence from the duct [9].

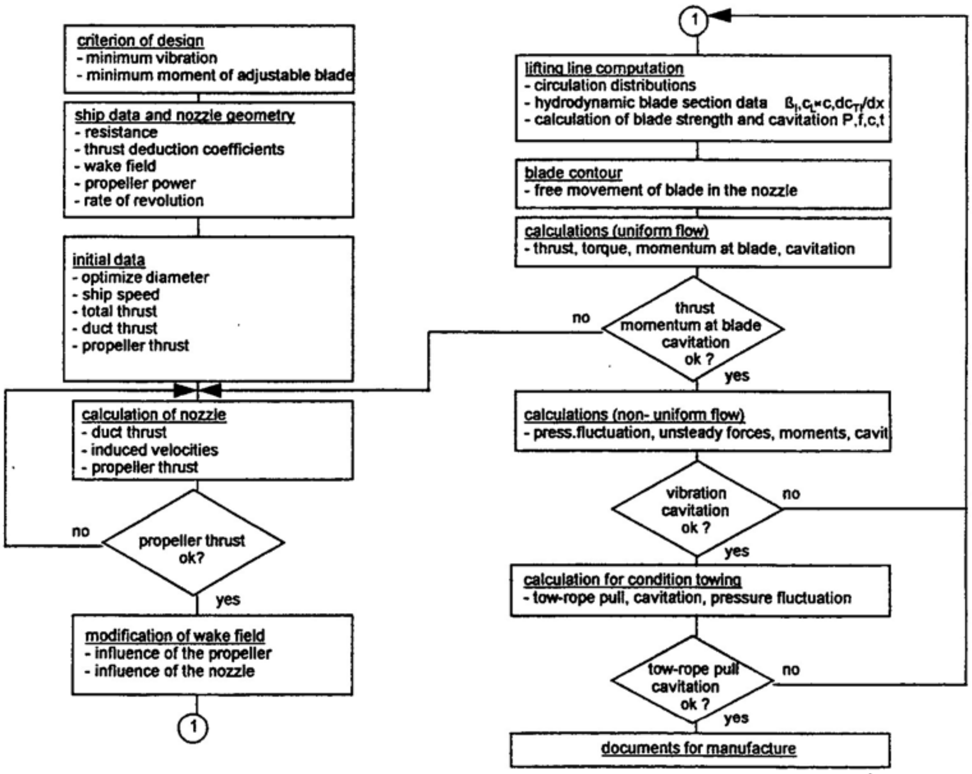

Fig. 2 Flow chart for ducted propeller design

The duct thrust and the velocity induction of the duct are calculated by a potential theory based on a vortex lattice model for the duct [10]. The direct vortex modelling Γ (x, y, z), the Biot-Savart operator and simple, suitable flow conditions are sturdy means for numerically stable solutions. As shown by the flow chart give in Figure 2 the design process is running iteratively in several loops. The emphasis of the present design task is the variation of the blade outline, characterised by the position Y/R of the chord centres of the profiles in the developed and expanded blade area representation.

A parabolic representation statement has proved to be successful:

$$y = Y/R = \left[x^2 - (x_1 + x_2)x + x_1x_2\right] * \frac{\tan\theta_{1.0}}{1-(x_1+x_2)+x_1x_2}$$

- x nondimensionalised blade section radius r/R
- x_1 nondimensionalised boss radius
- x_2 intersectional point of the curve of chord centres with the axis of rotation
- $\Theta_{1.0}$ angular position of the blade tip with respect to the axis of rotation

From the iterative design process run load distribution, propulsion efficiency during full speed and towing, setting momentums, cavitation during full speed and towing, excitation effect in the wake field are obtained and these resulted an optimum outline shape at $x_2 = 0.8$ and $\Theta_{1.0} = 15°$. This corresponds to an effective skew angle $\Theta_{eff} = 27.5°$. With respect to the design requirement of free movement of the set blades in the duct no fixing of a negative rake was necessary. Figure 3 shows a comparison of the blades of the conventional ducted propeller (CP 3029) and of the optimised design (CP 3031). The profile parameters of the optimised ducted propeller are illustrated in Figure 4 .

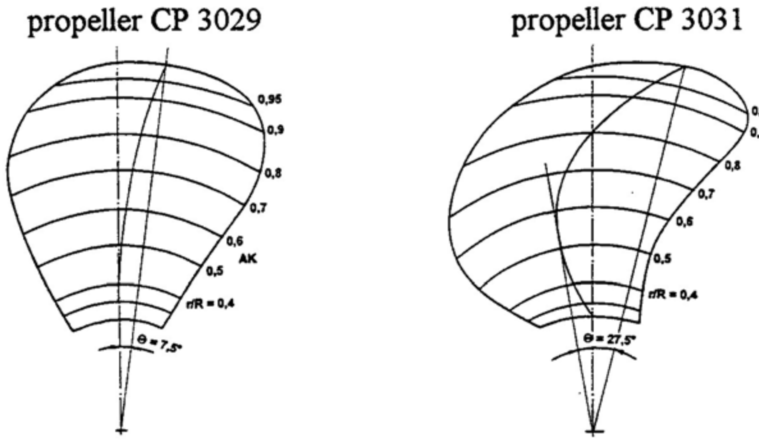

Fig. 3 Projected outline of the model propellers CP 3029 and CP 3031

The optimisation calculations of the blade shape with respect to the hydrodynamic effect of the ducted propeller system in the nominal wake field has been realised by adopting two potential theory based:

- The lifting surface method for propeller and duct DUNCAN modelled for unsteady flow [11].
- The lifting line method coupled with the duct calculation method DUESE together with area corrections from Det Norske Veritas NV570W for free propellers [12].

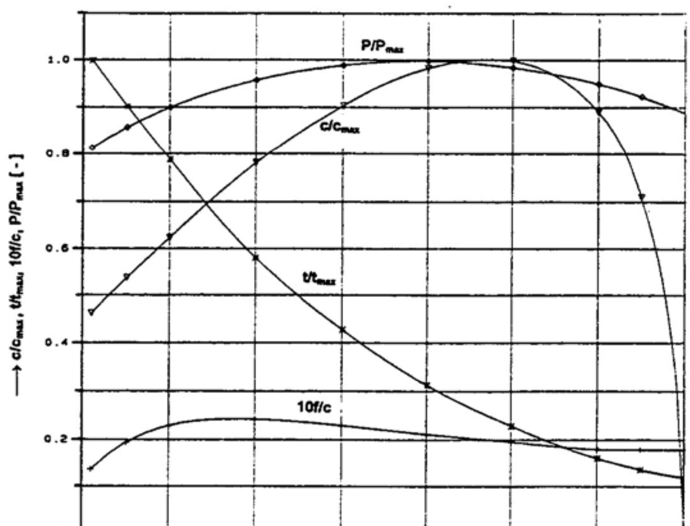

Fig. 4 Nondimensional propeller blade parameters

At the time of the design and at present, these methods for calculation of unsteady cavitation, pressure pulses and power fluctuations on ducted propellers constitute the advanced tool for the design engineer in industry. Absolute values are valid but to a limited extent only, but the trends in the hydrodynamic effects under variation of the geometry and inflow can be supposed to be useful. The Figures 5 and 6 show in comparison the results of the model test and calculation for pressure fluctuations and the extension of cavitation indicating the limits of the validity of the methods used.

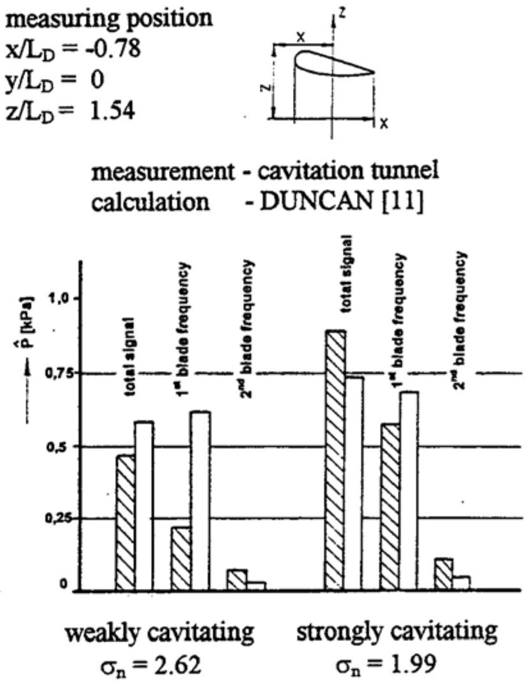

Fig. 5 Comparison of pressure fluctuations ducted model propeller CP 3031

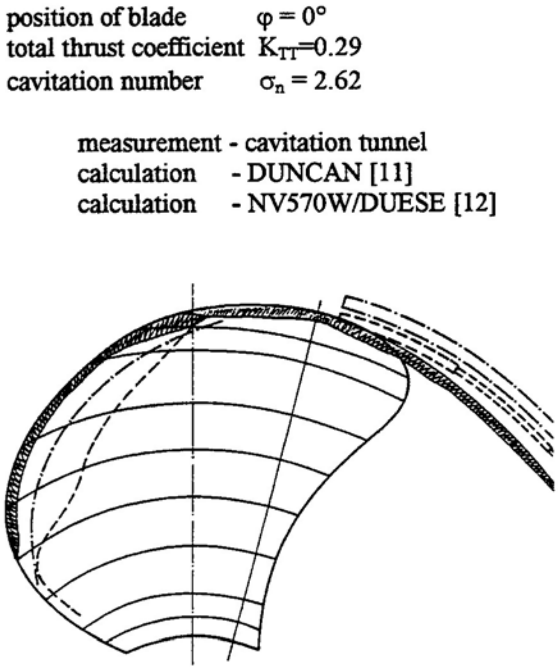

Fig. 6 Comparison of cavitation patterns ducted model propeller CP 3031

4. Experimental investigations

To examine the properties of ducted controllable pitch propellers, experimental investigations have been carried out by Schiffbau-Versuchsanstalt Potsdam on the conventional ducted propeller (model propeller CP 3029) and on the ducted propeller with higher blade skew (model propeller CP 3031).

Table 1: Data of the model propellers

Propeller N°:			CP 3029	CP 3031
Diameter	D	[m] :	0.252	0.252
Pitch ratio	$P_{0.7}/D$	[-] :	1.13	1.14
Pitch angle	$\phi_{0.7}$	[°] :	27.22	27.39
Area ratio	A_E/A_0	[-] :	0.600	0.575
Skew angle	Θ_{eff}	[°] :	7.40	27.50
Number of blades	z	[-] :	4	4

The ducts used both in full scale and in the model test were Wageningen 19A ducts. Table 2 shows the principal data of the model duct D122.

Table 2: Data of the model duct D122

Length of duct	L_D	[m] :	0.1275
Inner diameter	D_I	[m] :	0.2550
Entrance diameter	D_E	[m] :	0.3014
Leaving diameter	D_A	[m] :	0.2660
Position of propeller	x_P/D_I	[-] :	0.5

4.1 Thrust and torque measurements

Free runing tests under uniform inflow show that for a thrust loading coefficient corresponding to "full speed", designated by $K_{TT}/J^2 = 0.92$, model propeller CP 3031 with skewed blades features an efficiency η_0 better by about 2 % in comparison with the conventional model propeller CP 3029 (Figure 7).

Tests in the simulated wake field also confirm this result. The comparable thrust produced by model propeller CP 3031, characterised by the relation $K_{TT}/10K_Q$, in "full speed" condition is about 1 % higher than CP 3029 (Table 3).

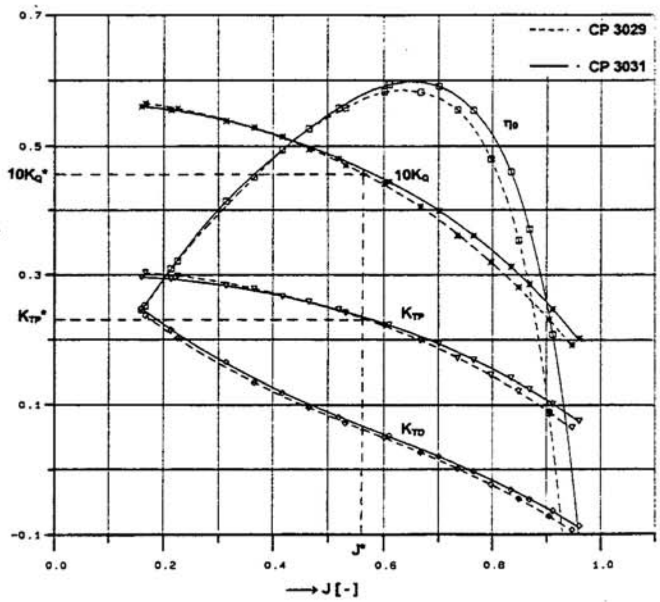

Fig. 7 Open water characteristics for ducted propellers CP 3029 and CP3031

Table 3: Propeller characteristics in the simulated wake field

Propeller	K_{TT}	$10K_Q$	$K_{TT}/10K_Q$	σ_n
CP 3029	0.294	0.457	0.643	13.56
CP 3029	0.293	0.457	0.641	2.60
CP 3031	0.303	0.465	0.652	13.56
CP 3031	0.301	0.465	0.647	2.60

Altogether, the investigations carried out show that for the actual thrust loading coefficients $C_{TH} = 2.34$ there is no distinct change of efficiencies that could be attributed to the choice of the blade shape.

4.2 Cavitation tests

The cavitation limits found out under uniform inflow for the condition "full speed" show that for model propeller CP 3031 with skewed blades, the tip vortex and sheet cavitation at the suction side begins earlier than for ducted propeller CP 3029. The character of the cavitation patterns is similar for both ducted propellers (Figure 8).

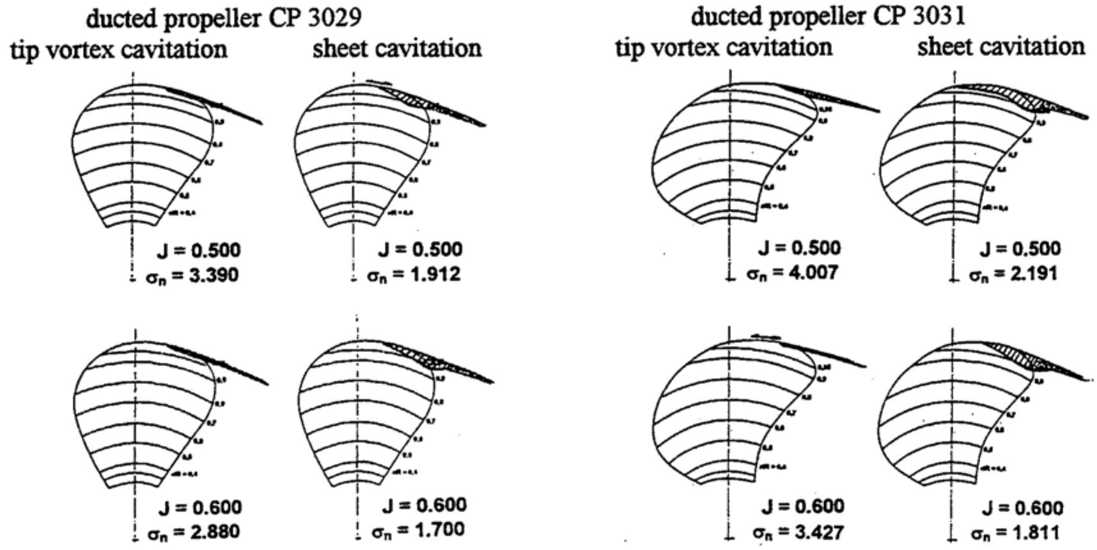

Fig. 8 Cavitation patterns for cavitation inception in uniform flow

In the simulated wake field, under the condition "full speed" and for the design cavitation number σ_n = 2.62 both propellers CP 3029 and CP 3031 produce pulsating tip vortex and suction side cavitation (Figure 9). For propeller CP 3031, cavitation remains effective over a larger angle range (φ = 300°... 0°... 80°), thus it does not pulsate as much as for CP 3029 (φ = 300° ... 0°... 60°).

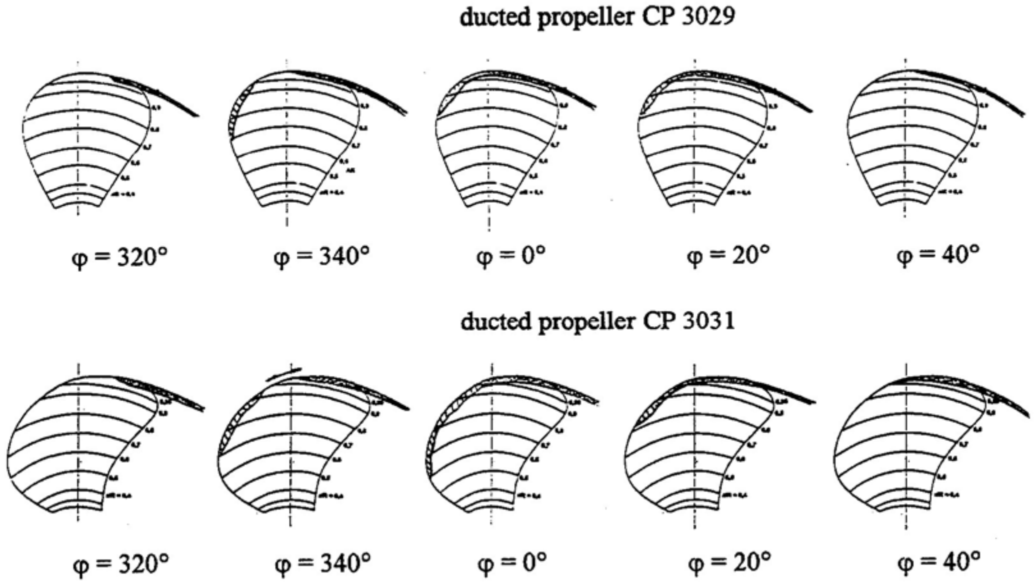

Fig. 9 Cavitation patterns in non-uniform flow for the design condition

In the towing condition, both ducted propellers feature tip vortex cavitation that remains effective without any essential pulsation over the whole blade rotation. No significant differences in the cavitation phenomena of both propellers had been observed.

4.3 Propeller induced pressure fluctuations

Propeller induced pressure fluctuations have been measured outside the duct at different measuring positions in response to the cavitation number. Table 4 illustrates the co-ordinates of the pressure pick-up points with respect to the model propeller.

Table 4: Co-ordinates for pressure fluctuation measurements

Position	x/L_D (forward positive)	y/L_D (starboard positive)	z/L_D (upwards positive)
1	0.500	0	1.228
2	1.055	0	1.228
3	-0.756	0	1.228

Coefficients were formed from the measured pressure fluctuation amplitudes $p_j^{(i)}$.

$$k_{pj} = \frac{p_j^{(i)}}{\rho * n^2 * D^2}$$

Figures 10 and 11 show the coefficients of pressure fluctuations of the 1st order for the conditions "full speed" and "towing" in response to the cavitation number σ_n for both investigated propeller variants.

In the cavitation-free state ($\sigma_n > 5.0$), increase of the skew angle of model propeller CP 3031 causes a decrease of the pressure fluctuation excitation. In front of the duct of the CP 3031, in condition "full speed" the pressure fluctuation amplitudes in the first blade frequency (4th number of revolutions order) are by about 15 % smaller than with model propeller CP 3029 (Figure 10). Behind the duct both propellers feature pressure fluctuations of identical magnitude. In the range of the practically interesting cavitation numbers the influence of cavitation on the pressure pulses already is distinctly present.

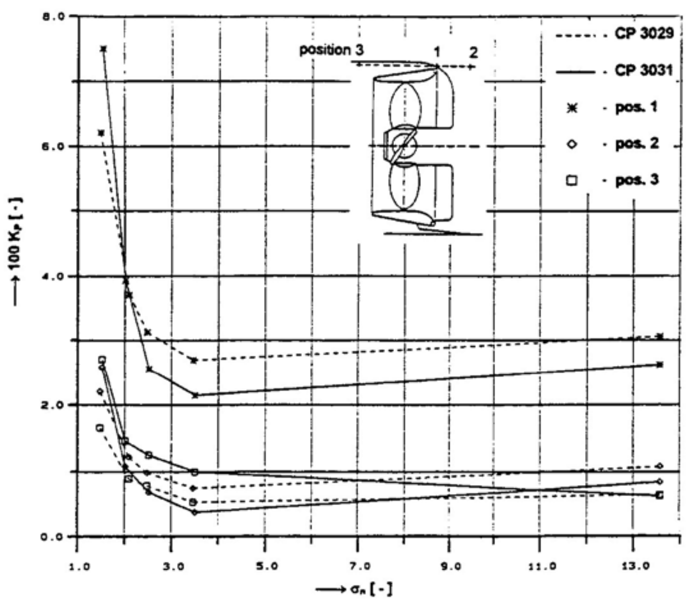

Fig. 10 Pressure fluctuation coefficients for the condition "full speed"

Now, the pressure fluctuations result from the displacement effect of the blades, from the (variable) circulation and from the pulsating cavitation. These portions differ from each other both in their amplitudes and also in their phase positions.

In front of the duct for the design cavitation number $\sigma_n = 2.62$ the ducted propeller CP 3031 induces lower pressure fluctuations. With increasing cavitation phenomena, beginning with cavitation numbers from $\sigma_n \leq 2.00$, ducted propeller CP 3031 will excite higher pressure fluctuations due to heavier cavitation suffered in comparison with ducted propeller CP 3029.

Model propeller CP 3031 induces a thicker cavitating tip vortex. Behind the duct higher pressure fluctuations are present than with ducted propeller CP 3029.

In condition "towing" the superiority of skewed propellers is clearer (Figure 11). The pressure fluctuation amplitudes of the first blade frequency are near the duct about 45 % smaller than with conventional propellers. Because under this condition the cavitation is but insignificant and scarcely pulsating, the reduction of pressure fluctuations chiefly is due to the higher skew angle.

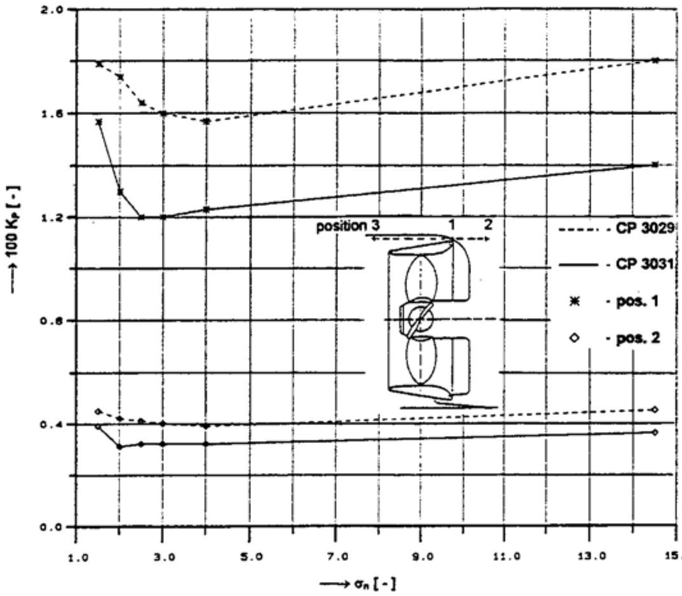

Fig. 11 Pressure fluctuation coefficients for the condition "towing"

4.4 Unsteady propeller forces and moments

Fluctuations have been measured in the bending moments on the individual blade occurring due to axial (thrust) and tangential (torque) force fluctuations in the wake and that are transmitted to the ship via the shaft and its bearing.

These measurements have been carried out only in the "full speed" condition considering that alternative propeller loads are decreasing in the "towing" condition and will disappear (theoretically) completely in pull during bollard test.

First of all it can be seen that the changes in propeller loading in the cavitation-free state and the design cavitation number differ but insignificantly (Figure 12).

The unsteady propeller forces and moments for the ducted propeller CP 3031 are lower than those of CP 3029 both in the cavitation-free state and for the design cavitation number in the number of revolutions orders n = 1 through 3. Altogether, the result of the analysis shows that the ducted propeller CP 3031 transmits lower unsteady propeller forces and moments to the shaft than the ducted propeller CP 3029.

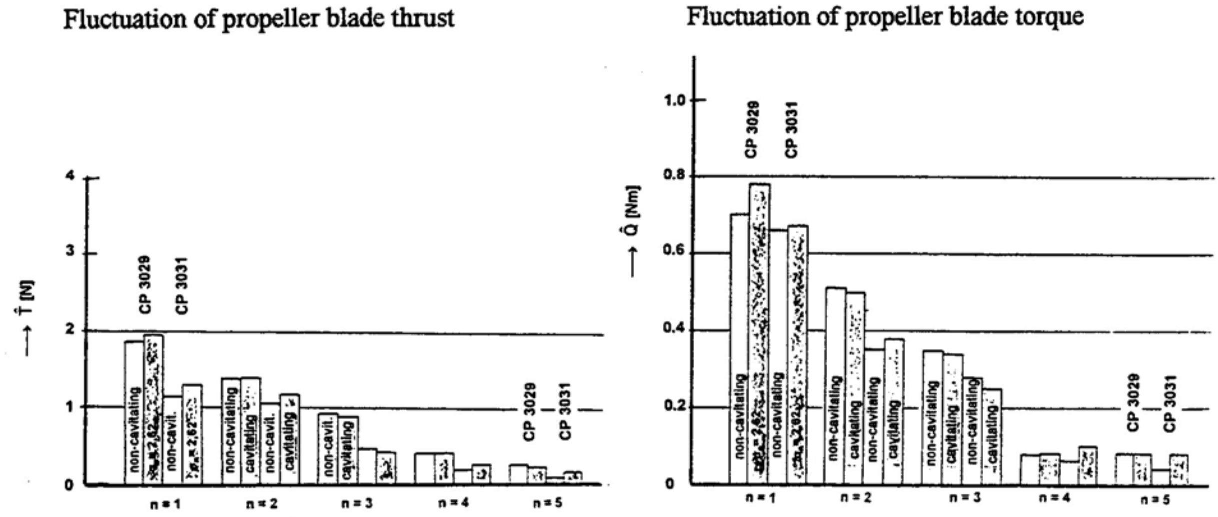

Fig. 12 Comparison of thrust and torque fluctuations on one blade

5. Conclusions

The results of comparative model investigations on ducted propellers for the fishing and processing trawler "ATLANTIK 488" show that a moderate increase of the effective blade skew of $\Theta_{eff} = 7.4°$ to $\Theta_{eff} = 27.5°$ provides the vessel with better properties in use than with a conventional blade outline.

Shifting the blade tip in to the propeller plane, a minimum gap between the blade tip and the inner jacket of the duct was guaranteed also during reversal of the controllable pitch propeller. The efficiency of the ducted propellers with skew will not be less than that of conventional ducted propellers.

The cavitation properties of propellers with higher blade skew differ but insignificantly in uniform inflow with respect to the cavitation inception and to the character of the cavitation developed. In non-uniform inflow, cavitation pulsates less on CP 3031 and the cavitation extend is somewhat greater and the cavitating tip vortex is more distinct.

For the cavitation-free and for the low-cavitating state the use of ducted propellers with higher blade skew presents a marked decrease in the propeller-excited pressure fluctuations.

Increase of the skew angle decreases the fluctuations of bending moments on the propeller blade and the load fluctuations transmitted to the shaft will be smaller.

The use of ducted propellers with moderate blade skew can be recommended both for fixed-pitch propellers and for controllable pitch propellers.

6. List of symbols

A_E/A_0	[-]	blade area ratio	
c	[m]	chord length of section	
C_{TH}	[-]	total thrust loading coefficient	$T_T/(0.5\rho\pi D^2/4V_A^2)$
D	[m]	diameter of propeller	
D_A	[m]	duct diameter at the leaving cross-section	
D_E	[m]	duct diameter at the entrance cross-section	
D_I	[m]	duct diameter at propeller location (x_p)	
d_N	[m]	boss diameter	
d_N/D	[-]	boss diameter ratio	
f	[m]	propeller blade camber	
g	[m/s²]	acceleration due to gravity	
J	[-]	advance coefficient	$V_A/(nD)$
K_Q	[-]	torque coefficient	$Q/(\rho n^2 D^5)$
K_{dK}	[-]	coefficient for thrust loading	
K_P	[-]	pressure fluctuation coefficient	
K_{TD}	[-]	duct thrust coefficient	$T_D/(\rho n^2 D^4)$
K_{TT}	[-]	total thrust coefficient	$T_T/(\rho n^2 D^4)$
K_{TP}	[-]	propeller thrust coefficient	$T_P/(\rho n^2 D^4)$
L_D	[m]	nozzle length	
n	[s^{-1}]	rate of revolution of propeller	
P	[m]	pitch of propeller	
P/D	[-]	pitch ratio of propeller	
$p_j^{(i)}$	[Pa]	pressure fluctuation amplitude	
$P_{0.7}$	[m]	pitch of propeller at r = 0.7R	
p_0	[Pa]	hydrostatic pressure	
p_V	[Pa]	vapour pressure	
Q	[Nm]	propeller torque	
r	[m]	local propeller radius	
R	[m]	propeller radius	D/2
t	[m]	propeller blade thickness	
T	[N]	propeller thrust	
T_D	[N]	duct thrust	
T_T	[N]	total thrust	
V_A	[m/s]	propeller advance speed	
x,y,z		coordinates	
x_P/D	[-]	propeller position	
z	[-]	number of blades	
ϕ	[°]	pitch angle	
η_0	[-]	propeller efficiency	$(JK_{TT})/2\pi K_Q)$
φ	[°]	angular position of propeller blade, $\varphi = 0°$ vertically upwards	
ν	[m²/s]	kinematic viscosity	
Θ_{eff}	[°]	skew angle	
ρ	[kg/m³]	density of water	
σ_n	[-]	cavitation number, based on rate of revolution	$(p_0-p_V)/(0.5\rho n^2 D^2)$
τ	[-]	thrust ratio	T_D/T_T

7. References

1. Loth, H.D. and others, (1988), Fabriktrawler Typ "ATLANTIK 488", Seewirtschaft 6

2. Björheden, K., (1981) Highly Skewed-Verstellpropeller, HANSA, 118/12

3. van Manen, J.D., (1962), Effect of radial load distribution on the performance of shrouded propellers", International Shipbuilding Progress, 93

4. Philipp, O. & Bednarzik, R. & Bußler, M. & Hilbert, G., (1990) Düsenverstellpropeller mit erhöhter Flügelrücklage, Patentschrift B 63 H 5/15

5. Schroeder, G., (1967), Wirkungsgrad von Düsenpropellern mit unterschiedlicher Düsen- und Propellerform, Schiffbautechnik, 8

6. Kompleks dvižitelnyj grebnoj vint-napravljajuščaja nasadka. Methodika rasčeta i pravila projektirovanija, Zweigspezifischer Standard OST 5.4129, Moskau, 1975

7. Philipp, O., (1980), Vorläufige Richtlinie für den Entwurf von Düsen-Verstellpropellern für Fischereischiffe, report VEB Dieselmotorenwerk Rostock, No. 90.000-2101

8. Schlüter, H.-J. & Busse, A., (1986), Berechnung der induzierten Fortschrittswinkel von Propellern mit Hilfe der Induktionsfaktormethode bei Berücksichtigung des Einflusses der Nabe und Ummantelung, Schiffbauforschung, 25/1

9. Paul, W., (1987), Wölbungs- und Anstellwinkelkorrekturen für ummantelte Schiffspropeller, Schiffbauforschung, 26/4

10. Nickel, R., (1984), Ein potentialtheoretisches Modell zur Berechnung der Umströmung von beliebigen nichtrotationssysmmetrischen Propellerdüsen in nichtrotationssymmetrischer stationärer Anströmung, Schiffbauforschung, 23/3

11. Szantyr, J.A.& Glover, E.J., (1988), The unsteady lifting surface program for analysis of ducted propellers in the non-uniform inflow field, Emerson Cavitation Tunnel Report No. 3/88

12. Wagner, K., (1984), Effektive Wechselbeziehung zwischen Erzeugnisforschung und Schiffbauversuchswesen - Voraussetzung für die Entwicklung optimaler Propulsionsanlagen, Schiffbauforschung, 23/3